Proceedings of 2015 IEEE
International Conference on Mechatronics and Automation
August 2 - 5, Beijing, China

Path Planning for Surface Inspection on a Robot-Based Scanning System

Qian Wu, Jinyan Lu, Wei Zou, De Xu
Research Center of Precision Sensing and Control
Institute of Automation, Chinese Academy of Sciences, Beijing, China
qian.wu@ia.ac.cn

***Abstract* - This paper proposes an automatic model-based path planning method for surfaces inspection on a robot-based scanning system. The original CAD model of the surface is a triangular mesh model. The scanning system consists of a 6 degree of freedom robot and a coded structured light scanner. Based on the system structure and the working conditions of the scanner, some scan constraints, i.e. field of view, working distance, view angle, and overlap, are concerned in path planning. The proposed method consists of four steps: model framework extraction, scan region segmentation, viewpoint generation, and scan path generation. Firstly, model framework is extracted from the projection of model in main direction. Secondly, the model is divided into several scan regions based on the framework. Thirdly, viewpoints satisfied scan constraints are planned for each scan region. Lastly, a scanning path is generated passing through these viewpoints. Experiments are presented to demonstrate the feasibility and advantages of the proposed method.**

Index Terms – Surface inspection. Path planning. Structured light scanner, Robot-based system.

I. INTRODUCTION

Nowadays, structured light based surface measurement technique has been wildly used in surface inspection, reverse engineering, cultural heritage, medicines, etc [1-4]. Compared with the Coordinate Measurement Machine (CMM), a typical contact-type surface measuring device, the structured light scanner is non-invasive, faster, and much less expensive [5]. Particularly, the newly developed coded structured light scanner has notably improved the scanning efficiency by replacing line scanning mode, which is applied in the line structured light scanner, with plane scanning mode. Therefore, the coded structured light has been used more and more widely in surface inspection. However, a scanner can only detect a portion of the object from a single viewpoint, when the object has large surface. Therefore, a moving platform is usually required to move the scanner or the object in an automatic scanning system. The scanning system studied in this paper consists of an industrial robot with 6 degree of freedom (DOF) and a coded structured light scanner. The scanner is mounted on the end of the robot.

Since multiple viewpoints are often required for an object scanning, path planning which generates scan viewpoints and a path through these viewpoints are critically important for full automatic and high efficient inspection. Usually, surface inspection is a model-based issue, where the CAD model of the scanned object is assumed to be known. In this paper, the surface model is given as a triangular mesh model for its advantages of simplicity and robustness.

Many previous research works on scanning path planning are related to other scanning devices, such as CMMs, laser scanners, and cameras. Lee et al. [6-8] proposed an automated path planning method for freeform shape part inspection using laser scanners. Five constraints were concerned in the method: view angle, field of view (FOV), depth of view, beam occlusion-free, and path occlusion-free. Elkott et al. [9] developed a sampling method based on genetic algorithm for freeform surface inspection planning using CMMs. Chen et al. [10] proposed an automatic viewpoint planning method for robot vision system, which is equipped with stereo vision sensors. All geometrical, optical, reconstructive, and environmental constraints were considered in this research. Fernandez et al. [11] developed an automatic viewpoint planning system for 3D surfaces scanning using a laser stripe system mounted on a CMM. Both laser system and CMM system constraints had been considered. Martinez et al. [12] developed a sensor planning system for headlamp lens inspection using cameras, considering constraints of visibility, FOV, resolution, focus, and view angle. Scott [13] proposed a modified measurability matrix path planning algorithm for object inspection with laser scanners. Zhou et al. [14] presented a search-based path planning method for freeform surface inspection Zhao et al. [15] developed a path planning method for multi-sensor system, where a laser line scanner is combined with a touch trigger probe.

This paper proposes an automatic model-based path planning method that can achieve high precision and efficiency for surface inspection on a robot-based scanning system. The planned path is linked by a group of viewpoints, from which the scanner can detect the full features of the object. In order to achieve high-precision measurement, each viewpoint should satisfy several scan constraints, i.e. FOV, working distance, view angle, and overlap. The proposed method is mainly composed by four steps: model framework extraction, scan region segmentation, viewpoint generation, and scanning path generation. Firstly, model framework is extracted through projection in main direction of the model. Secondly, the model is divided into several scan regions based on the framework. Thirdly, viewpoints satisfied scan constraints are planned for each scan region. Lastly, a scanning path is generated passing through these viewpoints. An airplane wing model is taken as an example in this paper. Experiment results demonstrate the feasibility and advantages of the proposed method.

II. System Description

The scanning system studied in this paper consists of a 6 DOF robot and a coded structured light scanner, as shown in Fig. 1. The scanner is mounted on the end of the robot. The followed four coordinate systems, i.e. robot base coordinate system, robot end coordinate system, scanner coordinate system, and object coordinate system, are established in the scanning system, as Fig. 2 shown.

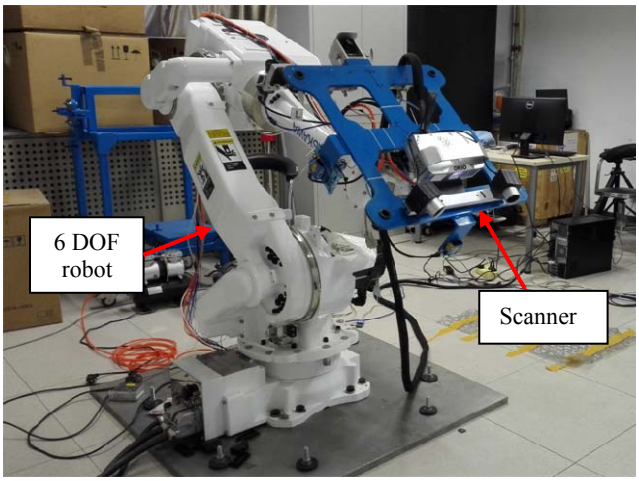

Fig. 1 Robot-based scanning system

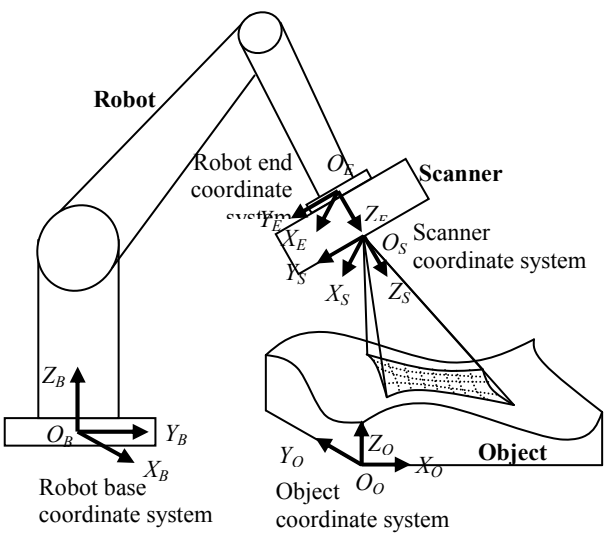

Fig. 2 Coordinate systems

In this paper, the viewpoint is planned based on the CAD model of the object. Thus, the viewpoint is defined by the position and pose of the scanner in the object coordinate system. Denote *VP* as the set of viewpoints.

$$VP:\left\{vp_i:\{{}^{O}\boldsymbol{R}_{Si},\,{}^{O}\boldsymbol{T}_{Si}\}\,\middle|\,i=1,\cdots,N_{VP}\right\}$$

where vp_i is a viewpoint. ${}^{O}\boldsymbol{R}_{Si}$ and ${}^{O}\boldsymbol{T}_{Si}$ are the rotation matrix and the position vector of the scanner in object coordinate system respectively, when the scanner is set at the viewpoint vp_i. N_{VP} is the number of the viewpoints.

The scanning path is defined as the path of the robot end, since it can be set by the robot controller easily. Denote *SP* as the scanning path.

$$SP:\left\{sp_i:\{{}^{B}\boldsymbol{R}_{Ei},\,{}^{B}\boldsymbol{T}_{Ei}\}\,\middle|\,i=1,\cdots,N_{VP}\right\}$$

where sp_i is a path point, ${}^{B}\boldsymbol{R}_{Ei}$ and ${}^{B}\boldsymbol{T}_{Ei}$ are the rotation matrix and the position vector of the robot end in robot base coordinate system respectively, when the robot end is set at the path point sp_i.

In the scanning path, the scanner will pass though these viewpoints. According to the system structure, the relationship between *VP* and *SP* is as follows

$$\begin{bmatrix} {}^{B}\boldsymbol{R}_{Ei} & {}^{B}\boldsymbol{T}_{Ei} \\ 0 & 1 \end{bmatrix} = \begin{bmatrix} {}^{B}\boldsymbol{R}_{O} & {}^{B}\boldsymbol{T}_{O} \\ 0 & 1 \end{bmatrix} \begin{bmatrix} {}^{O}\boldsymbol{R}_{Si} & {}^{O}\boldsymbol{T}_{Si} \\ 0 & 1 \end{bmatrix} \begin{bmatrix} {}^{E}\boldsymbol{R}_{S} & {}^{E}\boldsymbol{T}_{S} \\ 0 & 1 \end{bmatrix}^{-1} \quad (1)$$

where $\{{}^{B}\boldsymbol{R}_{O},\,{}^{B}\boldsymbol{T}_{O}\}$ is the pose and position of the object in the robot base coordinate system, $\{{}^{E}\boldsymbol{R}_{S},\,{}^{E}\boldsymbol{T}_{S}\}$ is the pose and position of the scanner in the robot end coordinate system .

III. Scan Constraints

Some scan constraints should be considered during path planning process. Firstly, the measured points should be within the working distance of the scanner. Secondly, the measured points should be located within the FOV of the scanner. Thirdly, overlap area is required for integrating data detected from different viewpoints. The followed parameters are related about above scan constraints:

1. Working distance range: $[H, H+h]$;
2. Smallest range of FOV: $l_1 \times w_1$;
3. Largest range of FOV: $l_2 \times w_2$;
4. Maximum acceptable view angle: θ_T;
5. Minimum acceptable width of overlap W_V.

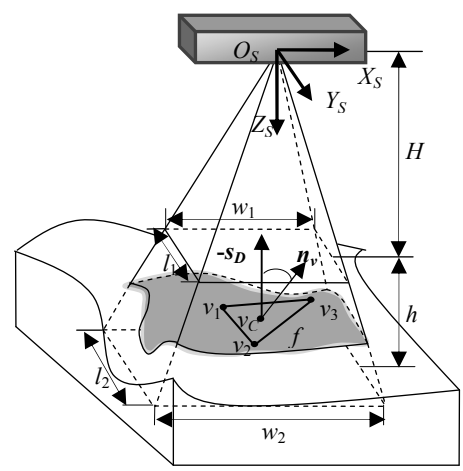

Fig. 3 Scanner constraints

In this paper, the CAD model is a triangular mesh model. As shown in Fig. 3, *f* is a triangular facet within the measured location of the scanner. Suppose v_1, v_2, v_3 are three vertexes of *f*, v_C is its centroid, and $\boldsymbol{n_v}$ is its normal vector. If the coordinates of v_1, v_2, v_3 in the scanner coordinate system are denoted as $({}^{S}x_1, {}^{S}y_1, {}^{S}z_1)$, $({}^{S}x_2, {}^{S}y_2, {}^{S}z_2)$, and $({}^{S}x_3, {}^{S}y_3, {}^{S}z_3)$ respectively, the coordinate of v_C can be calculated as:

$$({}^{S}x_C, {}^{S}y_C, {}^{S}z_C) = \left(\frac{1}{3}\sum_{i=1}^{3} {}^{S}x_i, \frac{1}{3}\sum_{i=1}^{3} {}^{S}y_i, \frac{1}{3}\sum_{i=1}^{3} {}^{S}z_i \right) \quad (2)$$

In summary, the constraints are given as follows:

(1) Working distance: the three vertexes should be within the working distance range, as Fig. 3 shown.

$$\begin{cases} H \le {}^{S}z_1 \le H + h \\ H \le {}^{S}z_2 \le H + h \\ H \le {}^{S}z_3 \le H + h \end{cases} \quad (3)$$

(2) FOV: the three vertexes should be located within FOV, as Fig. 3 shown.

$$\begin{cases} \left|{}^{S}x_1\right| \le \frac{{}^{S}z_1 w_1}{2H}, \left|y_1\right| \le \frac{{}^{S}z_1 l_1}{2H} \\ \left|{}^{S}x_2\right| \le \frac{{}^{S}z_2 w_1}{2H}, \left|y_2\right| \le \frac{{}^{S}z_2 l_1}{2H} \\ \left|{}^{S}x_3\right| \le \frac{{}^{S}z_3 w_1}{2H}, \left|y_3\right| \le \frac{{}^{S}z_3 l_1}{2H} \end{cases} \quad (4)$$

(3) View angle: The angle between negative unit vector of scan direction $\boldsymbol{s_D}$ and $\boldsymbol{n_v}$ should be less than θ_T , as shown in Fig. 3.

$$-\boldsymbol{s_D} \cdot \boldsymbol{n_v} \ge \cos\theta_T \quad (5)$$

where the direction of Z_S axis is the scan direction $\boldsymbol{s_D}$.

(4) Overlap: the width of overlap is larger than W_V, as shown in Fig. 4.

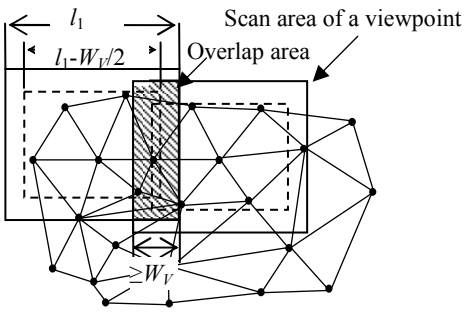

Fig. 4 Overlap constraint

IV. Path Planning Method

The data of triangular mesh model F consists of vertexes and normal vectors of facets.

$$F : \left\{ f_i : \{ v_{i1}, v_{i2}, v_{i3}, \boldsymbol{n_{vi}} \} \middle| i = 1, \cdots, N_F \right\}$$

Define a $1 \times N_F$ array M to record the statuses of facets.

$$M(i) = \begin{cases} 1; if\ f_i\ has\ been\ planned \\ 0; otherwise \end{cases} \quad (6)$$

The overall procedure of the proposed method consists of four steps: model framework extraction, scan region segmentation, viewpoint generation, and path generation, as shown in Fig. 5.

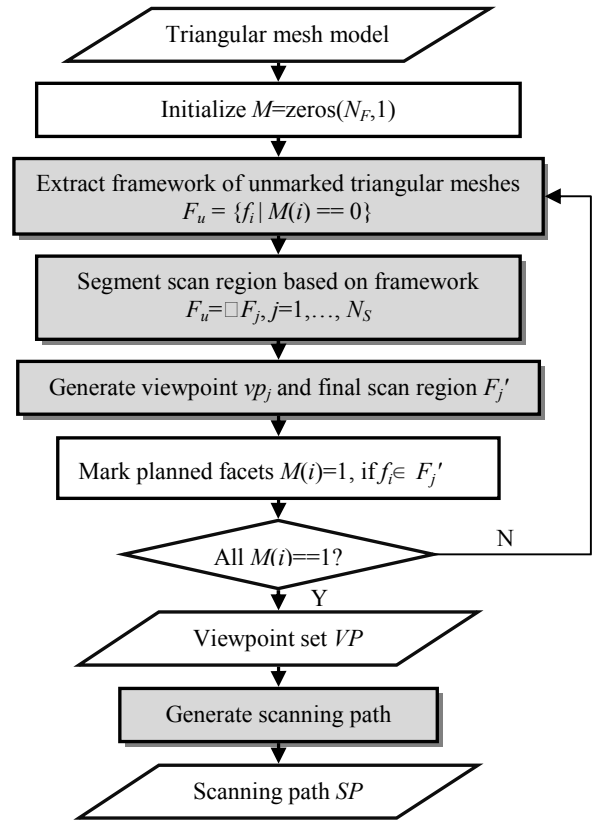

Fig. 5 Overall procedure of the path planning method

A. Model Framework Extraction

In this step, model framework is extracted through model projection in the main direction $\boldsymbol{n_m}$, which is determined by the global mean of the normal vectors in the model.

$$\boldsymbol{n_m} = -\frac{\sum_{j=1}^{N_F} \boldsymbol{n_{vj}}}{\left|\sum_{j=1}^{N_F} \boldsymbol{n_{vj}}\right|} \quad (7)$$

All the vertexes in the model are perpendicularly projected on to plane Π, which passes through the origin O_O and has the normal vector $\boldsymbol{n_m}$, as shown in Fig. 6. The projected points p_i of a vertex v_i is calculated as

$$p_i = v_i + (\overrightarrow{v_i O_o} \cdot \boldsymbol{n_m})\boldsymbol{n_m} \quad (8)$$

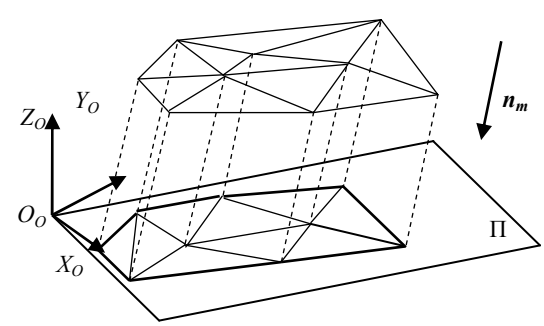

Fig. 6 Framework extraction

Denote pf_i as the projection of f_i, PF as the set of all facet projection. The contour of the projection is the framework of the model. Then, the minimum enclosing rectangle (MER) of

the framework is generated by rotation method [16]. MER is defined as

$$MER : l_{MER} \times w_{MER} \tag{9}$$

where

$$\begin{aligned} S_{MER} &= l_{MER} \times w_{MER} \\ &= \min S_{rect} \qquad PF \subset S_{rect} \\ &= \min(l_{rect} \times w_{rect}); \end{aligned} \tag{10}$$

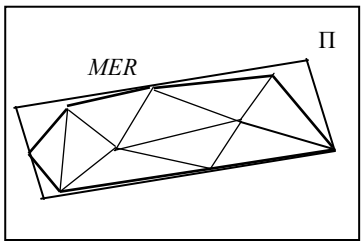

Fig. 7 MER extraction

B. Scan Region Segmentation

In this step, the model is divided into several scan regions based on the framework. Taking the smallest range of FOV and overlap constraint into consideration, a rectangle R_U with the size of $(l_1 - W_V/2)\times(w_1 - W_V/2)$ is set as the basic unit of framework segmentation. The segmentation of framework is as shown in Fig. 8. The framework is divided into N_S portions.

$$N_S = ceil\left(\frac{l_{MER}}{l_1 - W_V/2}\right) \times ceil\left(\frac{w_{MER}}{w_1 - W_V/2}\right) \tag{11}$$

where *ceil*() is a round up function to an integer. Denote R_j as a portion of the framework. Accordingly, the model is divided into N_S scan regions. Denote F_j as a scan region. F_j is defined as

$$F_j : \{f_j \mid p_{cj} \in R_j\} \tag{12}$$

where p_{cj} is the projection of f_j's centroid.

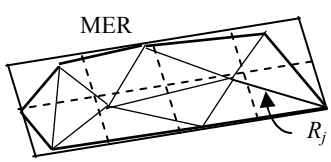

Fig. 8 Framework segmentation

C. Viewpoint Generation

In this step, viewpoints satisfied scan constraints are planned for each scan region. The scan direction $\boldsymbol{s_D}$ is determined by the global mean of the normal vectors in F_j.

$$\boldsymbol{s_D} = -\frac{\sum_{f_k \in F_j} \boldsymbol{n_{vk}}}{\left|\sum_{f_k \in F_j} \boldsymbol{n_{vk}}\right|} \tag{13}$$

All the vertexes in F_j are perpendicularly projected onto plane Π_j, which passes through the origin O_O and has the normal vector $\boldsymbol{s_D}$. The projected point p_{ij} of a vertex v_i is calculated as

$$p_{ij} = v_i + (\overrightarrow{v_i O_o} \cdot \boldsymbol{s_D})\boldsymbol{s_D} \tag{14}$$

Then, MER of the projections is generated by rotation method. Denote M_j as the MER, P_{MCj} as the centroid of M_j, P_{R1}, P_{R2}, P_{R3}, P_{R4} as the four vertexes of M_j, as Fig. 9 shown. Thus, the rotation matrix of this viewpoint is given as

$$^{O}\boldsymbol{R}_S = \left[\left(\frac{\overrightarrow{P_{R1}P_{R4}}}{\left|\overrightarrow{P_{R1}P_{R4}}\right|}\right) \quad \left(\frac{\overrightarrow{P_{R1}P_{R2}}}{\left|\overrightarrow{P_{R1}P_{R2}}\right|}\right) \quad \boldsymbol{s_D}\right] \tag{15}$$

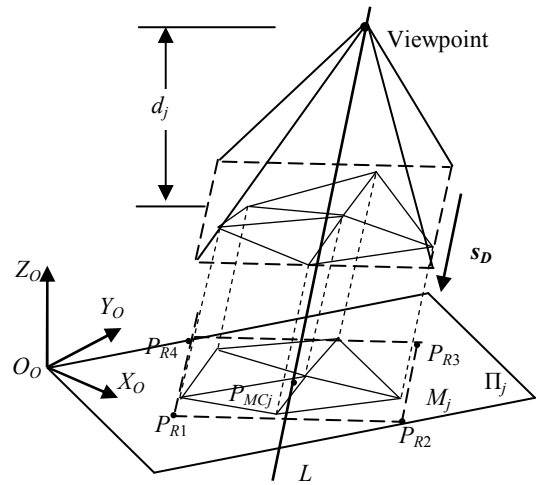

Fig. 9 Viewpoint generation

Taking overlap constraint into account, the FOV range of this viewpoint is set as

$$FOV : \left(\left|\overrightarrow{P_{R1}P_{R4}}\right| + \frac{W_V}{2}\right) \times \left(\left|\overrightarrow{P_{R1}P_{R2}} + \frac{W_V}{2}\right|\right)$$

According to the relationship between the working distance and FOV range of the scanner, the working distance d_j of this viewpoint is given as

$$\begin{aligned} d_j = \max\Bigg(&\max\left(\left|\overrightarrow{P_{R1}P_{R4}}\right| + \frac{W_V}{2}, \overrightarrow{P_{R1}P_{R2}} + \frac{W_V}{2}\right)\frac{H}{w_1}, \\ &\min\left(\left|\overrightarrow{P_{R1}P_{R4}}\right| + \frac{W_V}{2}, \overrightarrow{P_{R1}P_{R2}} + \frac{W_V}{2}\right)\frac{H}{l_1}\Bigg) \end{aligned} \tag{16}$$

All vertexes in F_j are perpendicularly projected onto line L, which passes through P_{RC} and is parallel to $\boldsymbol{s_D}$, as shown in Fig. 9. The projected point $p^L{}_i$ of a vertex v_i is calculated as

$$p^L{}_i = P_{RC} - \left(\overrightarrow{v_i P_{RC}} \cdot \boldsymbol{s_D}\right)\boldsymbol{s_D} \tag{17}$$

Denote PA^L as the set of all projected points. Then the top projected point $P^L{}_{top}$ in PA^L can be searched as

$$\overrightarrow{P_{RC}p^L{}_{top}} \cdot \boldsymbol{s_D} = \min_{p^L{}_i \in PA^L} \overrightarrow{P_{RC}p^L{}_i} \cdot \boldsymbol{s_D} \tag{18}$$

Then, the position of viewpoint is calculated as:

$$^{O}\boldsymbol{T}_S = p^L{}_{top} - d_j \cdot \boldsymbol{s_D} \tag{19}$$

So far, the viewpoint for scan region F_j has been generated.

Lastly, the view angle constraint is utilized to determine the final scan region F_j' of the current viewpoint. All the facets in F_j are checked by the view angle constraint in accordance with (5). Then, F_j' is given as

$$F_j' = \bigcup_{-\boldsymbol{S_D}\cdot\boldsymbol{n}_{vk} \geq \cos\theta_T} \{f_k\}; f_k \in F_j \tag{20}$$

Mark all facets in F_j'

$$M(i) = 1; if\ f_i \in F_j' \tag{21}$$

When the viewpoint set *VP* is generated by the previous steps, the scanning path *SP* passing though these viewpoints can be generated by (1).

V. Experiments

The proposed method was tested through an airplane wing surface. The surface model was shown in Fig. 10, which contained 14823 facets. The specification of scan constraints was given in Table I. The path planning method was implemented in MATLAB.

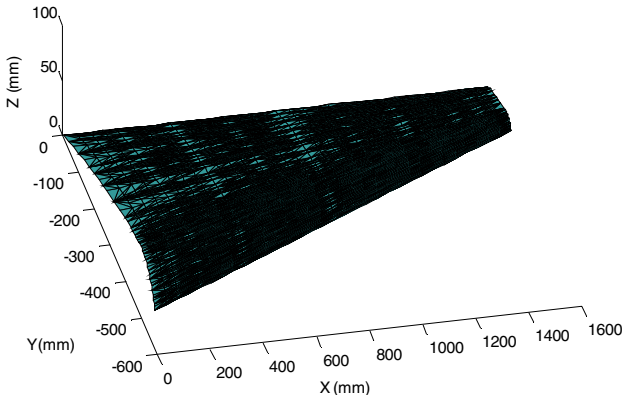

Fig. 10 Triangular mesh model of airplane wing surface

Table I Scan constraints

Parameter	Value
Smallest range of FOV	300 mm × 240 mm
Largest range of FOV	480 mm × 380 mm
Working distance range	0.5 m – 0.8 m
Maximum acceptable view angle	45°
Minimum acceptable width of overlap	40 mm

The model framework was extracted as shown in Fig. 11. The black polygonal represented the model framework. The blue rectangle represented MER. The green lines indicated the region segmentation. Thus, the model was divided into 18 regions. However, some region contained none facets.

Through viewpoints generation step, a viewpoint set including 13 viewpoints was obtained. The viewpoints and scan regions were shown in Fig. 12. Then, a scanning path was generated by (1). The planned path was adopted by the robot-based scanning system for an airplane wing inspection, as shown in Fig. 13. The scanned model of the airplane wing was shown in Fig. 14.

The software Geomagic was adopted to calculate the difference between the scanned model and the CAD model. The interface of software was shown in Fig. 15. The calculation results were shown in Fig. 16. The maximum difference was 15.1mm, the standard difference was 3.7 mm.

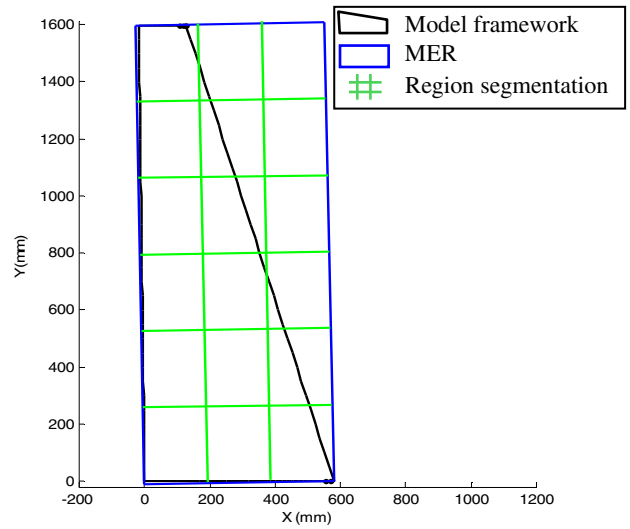

Fig. 11 Framework extraction

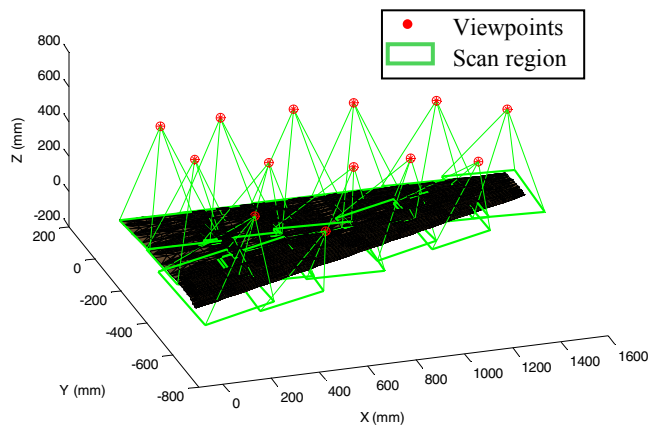

Fig. 12 Framework extraction

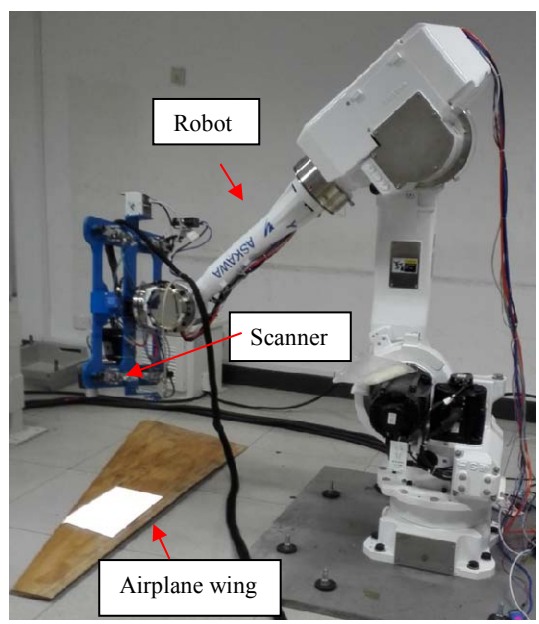

Fig. 13 Surface scanning system

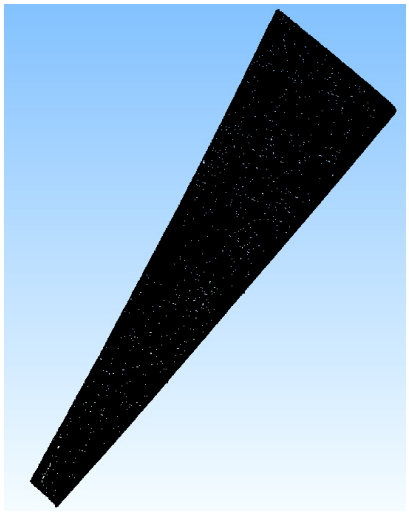

Fig. 14 Scanned model of airplane wing surface

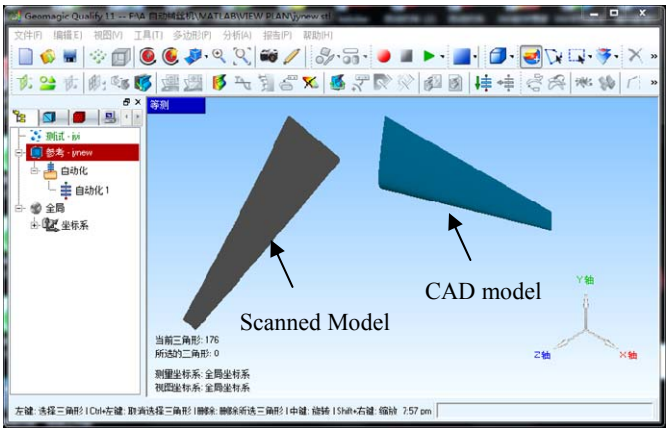

Fig. 15 Interface of Geomagic software

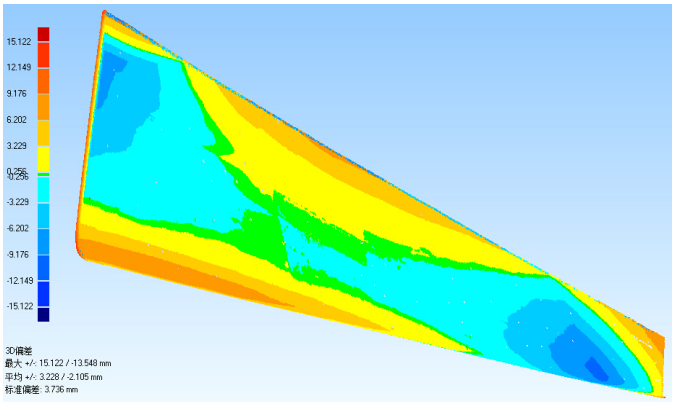

Fig. 16 Inspection results of airplane wing surface

It can be found from the experimental results that the planned path is reasonable and the surface inspection accuracy in experiment is satisfactory.

V. Conclusions

This paper proposed an automatic model-based path planning for surfaces inspection based on the robot-based scanning system. The utilization of triangular mesh model enables that the proposed method can be applied to any shape of objects. The four constraints, i.e. FOV, working distance, view angle, and overlap, are considered to guarantee the effectiveness of the planned viewpoints. An airplane wing is taken as an example in this paper. A scanning path for the airplane wing surface is planned by the proposed method. The experiment results demonstrate that the robot-based scanning system detects all feature of the airplane wing through the planned path.

References

[1] H. C. Nguyen, B. R. Lee, "Laser-vision-based quality inspection system for small-bead laser welding," *Int. J. Precis. Eng. Manuf.*, vol. 15, no. 3, pp. 415-423, 2014.

[2] E. Vezzetti, "Adaptive sampling plan design methodology for reverse engineering acquisition," *Int. J. Adv. Manuf. Technol.*, vol. 42, no. 7-8, pp. 780-792, 2009.

[3] G. Pavlidis, A. Koutsoudis, F. Arnaoutoglou, et al, "Methods for 3D digitization of cultural heritage," *Journal of Cultural Heritage,* vol. 8, no. 1, pp. 93-98, 2007.

[4] D. J. Yoo, "Three-dimensional human body model reconstruction and manufacturing from CT medical image data using a heterogeneous implicit solid based approach," *Int. J. Precis. Eng. Manuf.*, vol. 12, no. 2, pp. 293-301, 2011.

[5] Y. Fu, Y. Wang, M. Wan, et al, "Three-dimensional profile measurement of blade based on surface structured light," *Optik – International Journal for Light and Electron Optics*, vol.124, no. 8, pp. 3225-3229, 2013.

[6] K. H. Lee, H. P. Park, "Automated inspection planning for free-form shape parts by laser scanning. *Robotics and Computer Integrated Manufacturing*, vol. 16, no. 4, pp. 201-210, 2000.

[7] S. Son, K. H. Lee, "Automated scan plan generation using STL meshes for 3D stripe-type laser scanner," *In Computational Science and Its Applications — ICCSA 2003*, Springer Berlin Heidelberg, pp 741-750, 2003.

[8] S. Son, S. Kim, K. H. Lee, "Path planning of multi-patched freeform surfaces for laser scanning," *Int. J. Adv. Manuf. Technol.*, vol. 22, no. 5-6, pp. 424-435, 2003.

[9] D. F. Elkott, H. A. Elmaraghy, W. H. Elmaraghy, "Automatic sampling for CMM inspection planning of free-form surfaces," *International Journal of Production Research*, vol. 40, no. 11, pp. 2653-2676, 2002.

[10]S. Y. Chen, Y. F. Li, "Automatic sensor placement for model-based robot vision," *IEEE Transactions on System, Man, and Cybernetics—PART B: Cybernetics*, vol. 34, no. 1, pp. 393-408, 2004.

[11]P. Fernandez, J. C. Rico, B. J. Alvarez, et al, "Laser scan planning based visibility analysis and space partitioning techniques," *Int. J. Adv. Manuf. Technol.*, vol. 39, no. 7-8, pp. 699-715, 2008.

[12]S. S. Martinez, J. G. Ortega, J. G. Garcia, et al, "A sensor planning system for automated headlamp lens inspection," *Expert Systems with Applications*, vol. 36, no. 5, pp. 8768-8777, 2009.

[13]W. R. Scott, "Model-based view planning," *Machine Vision and Applications*, vol. 20, no. 1, pp. 47-69, 2009.

[14]A. Zhou, J. Guo, W. Shao, "Automated inspection planning of freeform surfaces for manufacturing applications," *In Proceedings of the 2011 IEEE International Conference on Mechatronics and Automation*, IEEE, Beijing, pp 2264-2269, 2011.

[15]H. Zhao, J. Kruth, N. V. Gestel, et al, "Automated dimensional inspection planning using the combination of laser scanner and tactile probe," *Measurement*, vol. 45, no. 5, pp. 1057-1066, 2012.

[16]N. Jiang, W. Yang, L. Duan, et al. "Acceleration of CT reconstruction for wheat tiller inspection based on adaptive minimum enclosing rectangle," *Computers and Electronics in Agriculture*, vol. 85, no. 5, pp.123–133, 2012.